CI2 – Inviscid Strong Vortex-Shock Wave Interaction


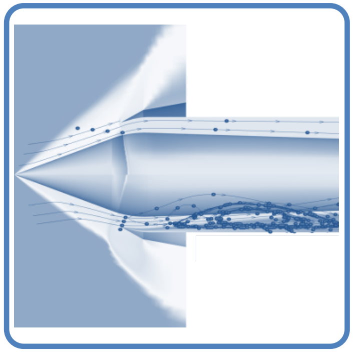
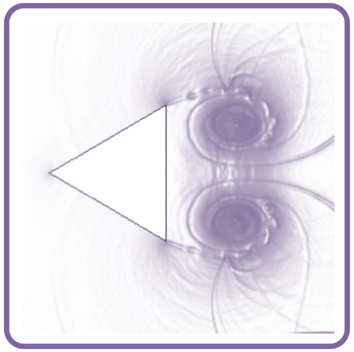

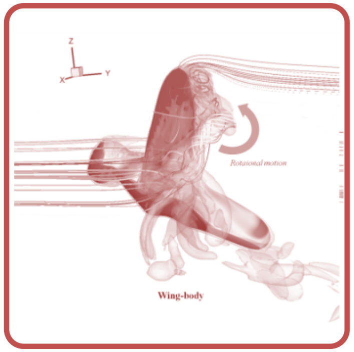

Hojun You*, Seonghun Cho and Chongam Kim

Department of Mechanical and Aerospace Engineering

Seoul National University, Korea

Jan. 6-7, 2018

Computations with In-house Solver

- **Seoul National University**
  - **Spatial discretization**
    - Discontinuous Galerkin method on high-order curved and mixed meshes
    - Orthonormal basis polynomials are constructed on physical domain.
  - **Temporal discretization**
    - Explicit TVD-RK3 for $P1$ and $P2$ approximations
    - Explicit 4th-order 5-stage SSP-RK for $P3$ approximation
  - **Shock capturing methods**
    - Hierarchical MLP (*h*MLP)[**Park and Kim, 2014**] (tagged as **SNU1** in the following figures)
    - Hierarchical MLP with Boundary Detector (*h*MLP_BD)[**You and Kim, 2017**] (tagged as **SNU2** in the following figures)
    - In non-simplex elements, simplex decomposition method is applied into both *h*MLP and *h*MLP_BD [**You and Kim, 2017**].
  - **Numerical flux**
    - Local Lax-Friedrich flux for VI1
    - Roe solver for CI2
  - **Implementation**
    - C++ language with Object-Oriented Programming (OOP)
    - Message Passing Interface (MPI)

Results

- **VI1**
  - **Total 76 (Slow vortex) + 81 (Fast vortex) cases**
    - Approximation order: $P1$, $P2$ and $P3$
    - Shock-capturing algorithm: no limiter, hMLP and hMLP_BD (with simplex-decomposition)
    - Meshes: RT, RQ with $1/h$ = 16, 32, 64, 128, 256
  - **Parallel computation**
    - Machine: Intel Xeon E5-2650 v4
    - MPI with 4 processors ($1/h$ =16, 32) and 24 processors ($1/h$ =64, 128, 256)
- **CI2**
  - **Total 96 cases**
    - Approximation order: $P2$ and $P3$
    - Shock-capturing algorithm: hMLP and hMLP_BD (with simplex-decomposition)
    - Meshes: RT, IT, RQ, M with $1/h$ = 50, 100, 150, 200, 250, 300

      ➔ $2\times2\times4\times6 = 96$
  - **Parallel computation**
    - Machine: Intel Xeon E5-2650 v4
    - MPI with one-hundred processors

Verification Test (VI1 – Inviscid Convected Vortex)

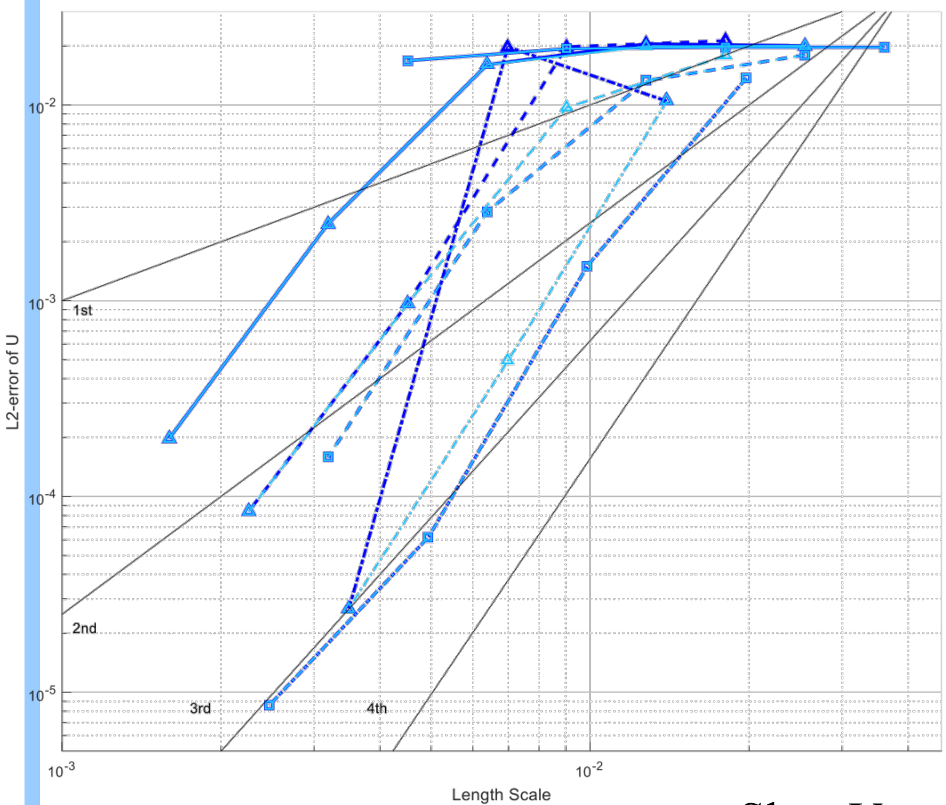

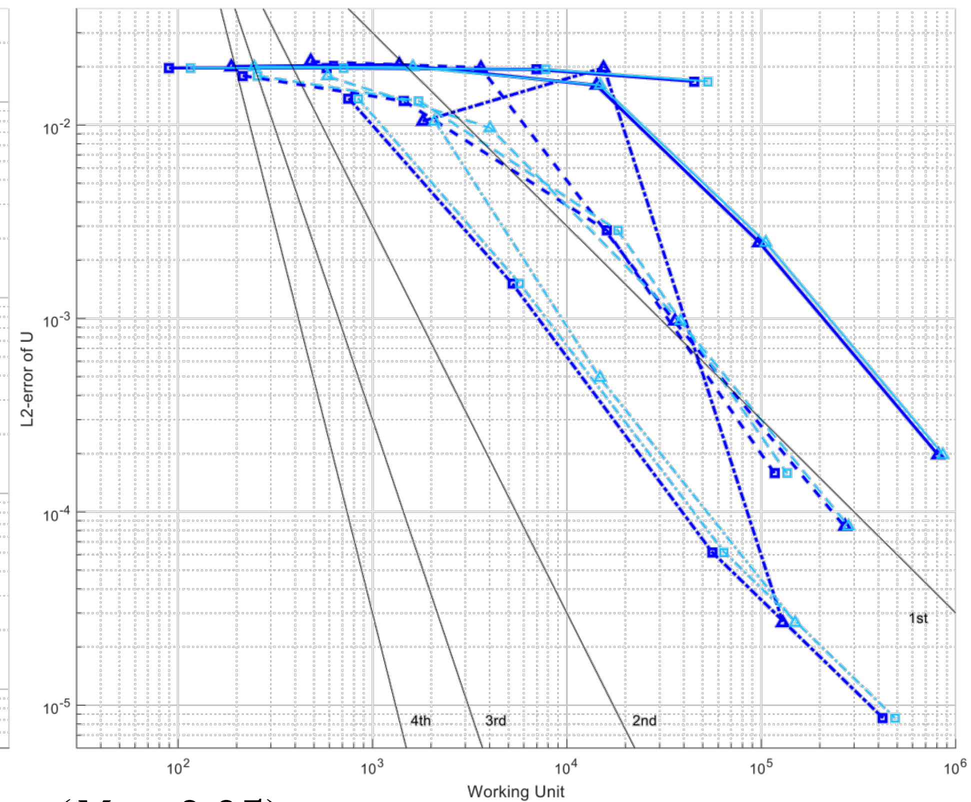

Slow Vortex ($M = 0.05$)

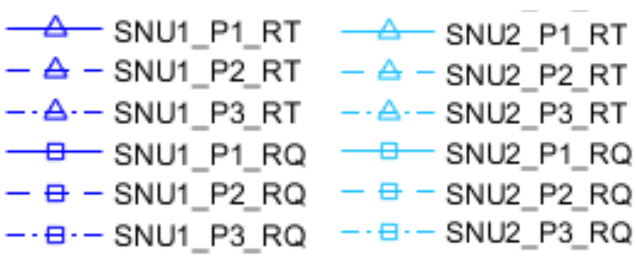

$$Error \sim O(h^{n+1})$$

$$Cost \sim O(h^2 \cdot h)$$

$$Error \sim O(Cost^{\frac{n+1}{3}})$$

Verification Test (VI1 – Inviscid Convected Vortex)

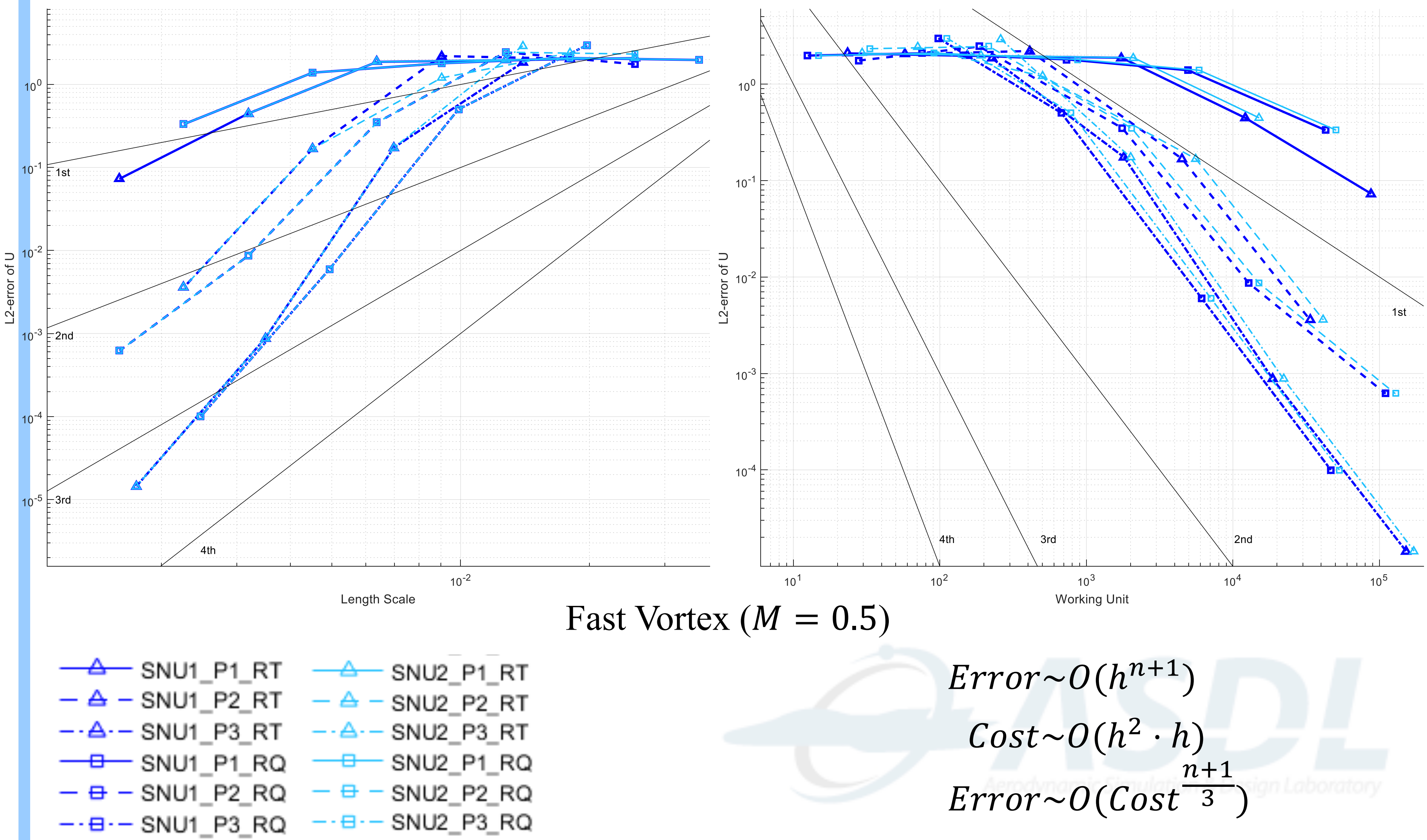

Fast Vortex ($M = 0.5$)

$$Error \sim O(h^{n+1})$$

$$Cost \sim O(h^2 \cdot h)$$

$$Error \sim O(Cost^{\frac{n+1}{3}})$$

Results (Schlieren View)

- **Effects of numerical flux**

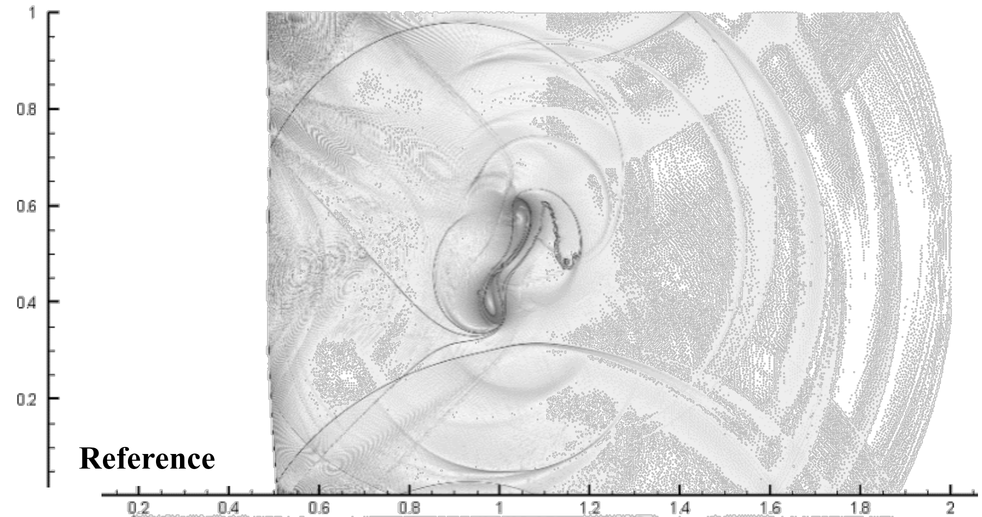

Reference

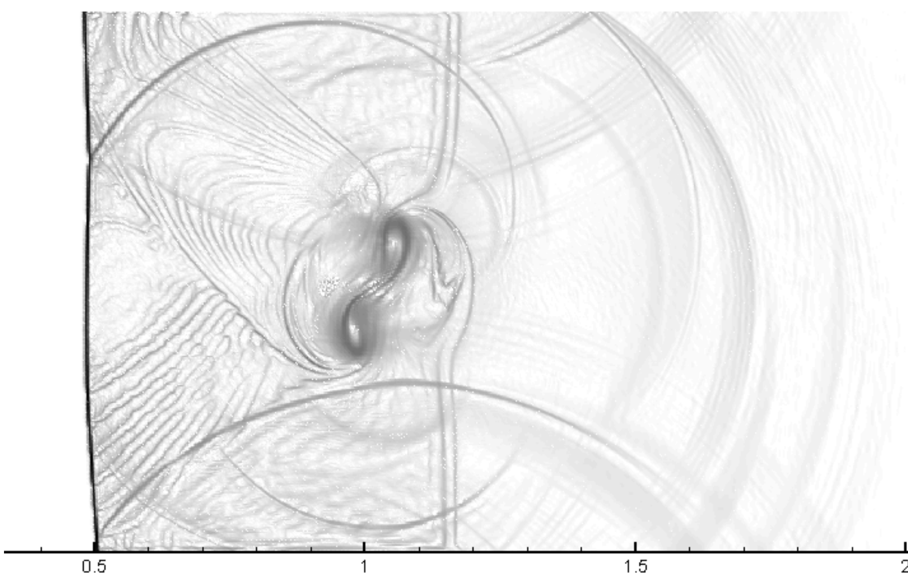

SNU2_P2_RT300 with LLF Flux

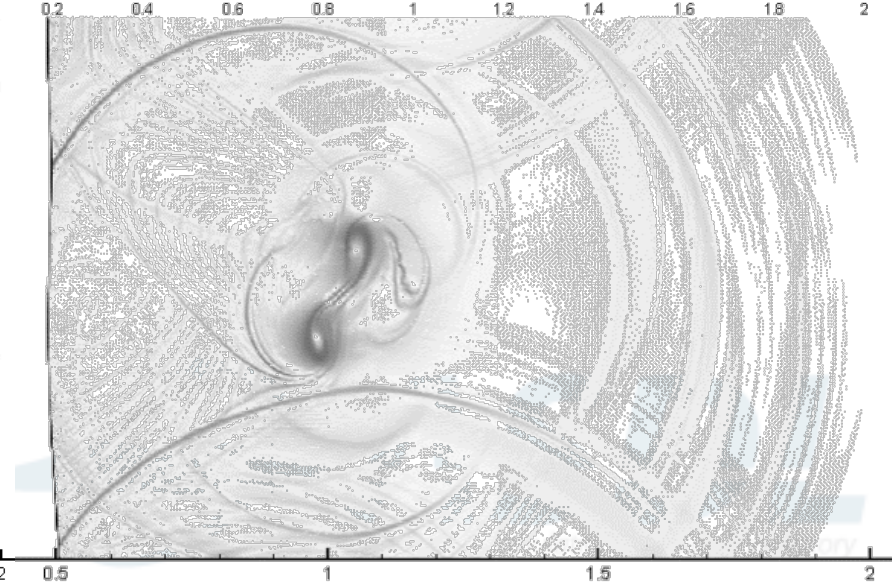

SNU2_P2_RT300 with Roe Flux

- **Effects of shock capturing method (SNU1 = *h*MLP, SNU2 = *h*MLP_BD)**

Reference

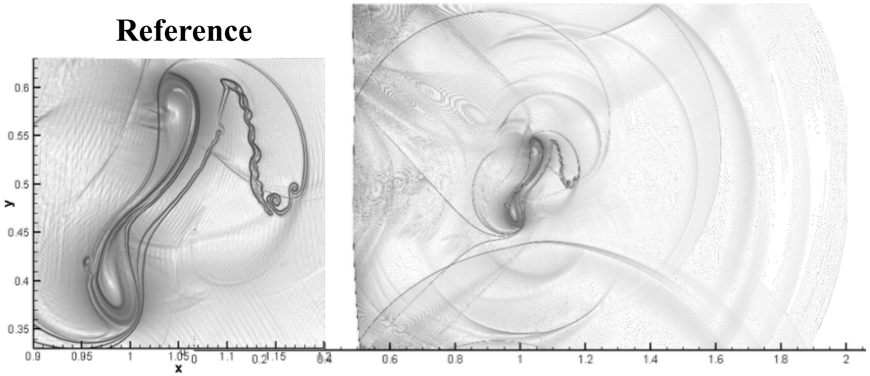

SNU1_P2_RT300

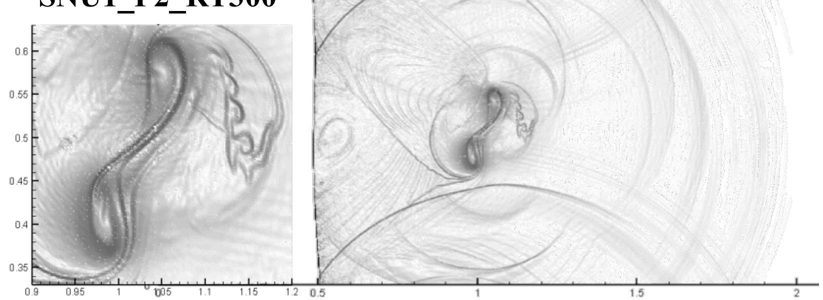

SNU2_P2_RT300

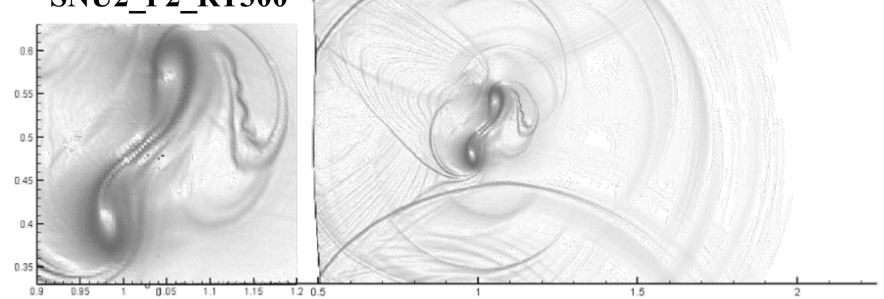

SNU1_P2_M300

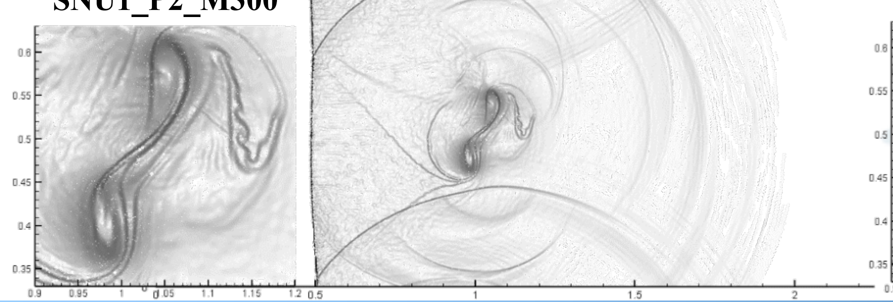

SNU2_P2_M300

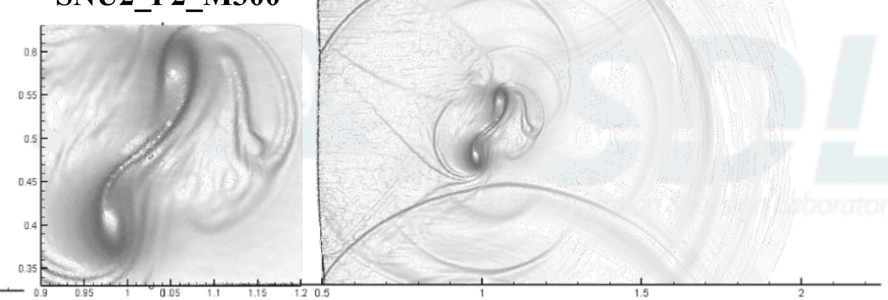

Results (Schlieren View)

- **Effects of approximation order**

Reference

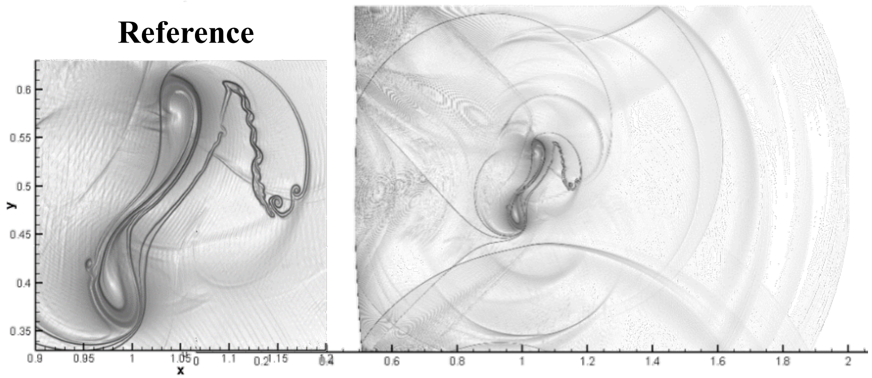

SNU1_P2_IT300

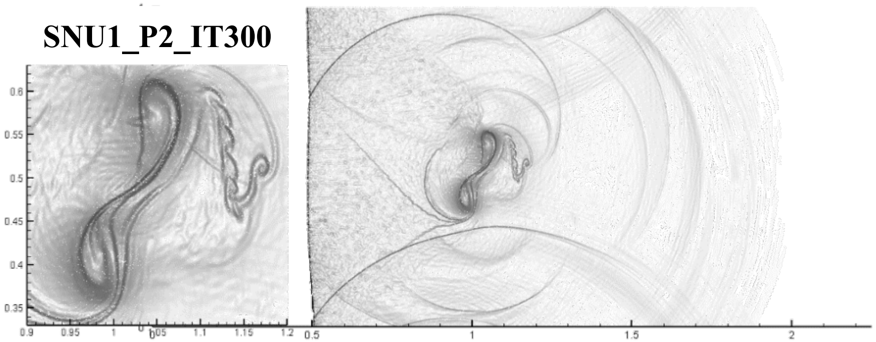

SNU1_P3_IT300

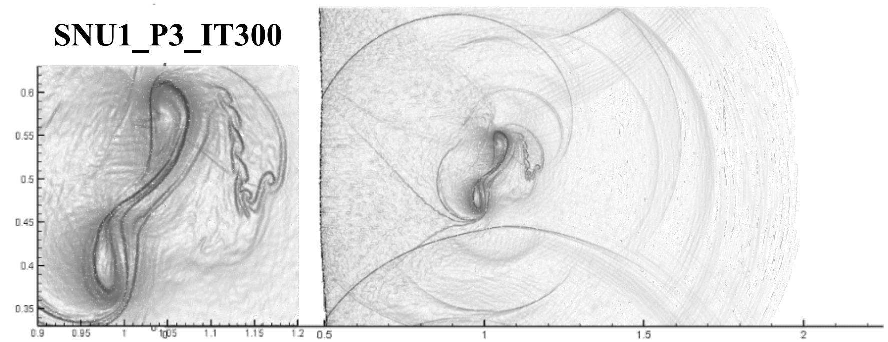

SNU2_P2_IT300

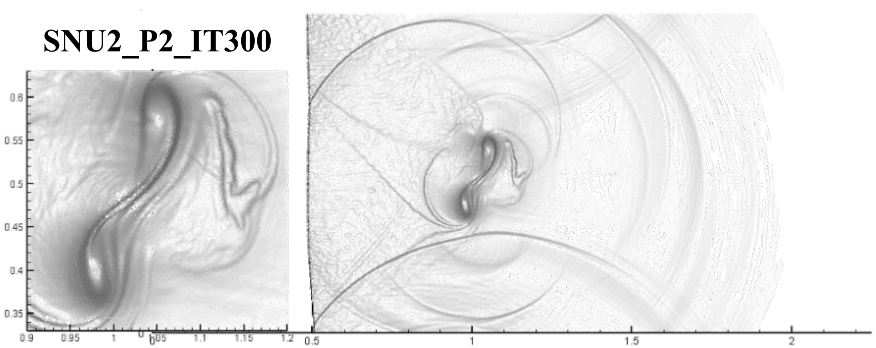

SNU2_P3_IT300

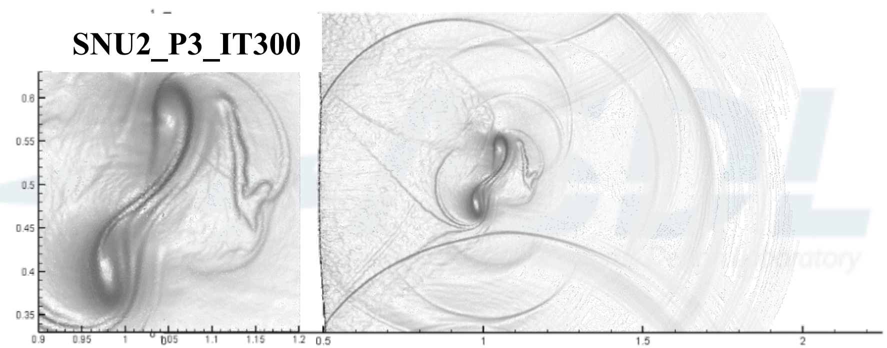

Results (Schlieren View)

- **Effects of mesh types**

Reference

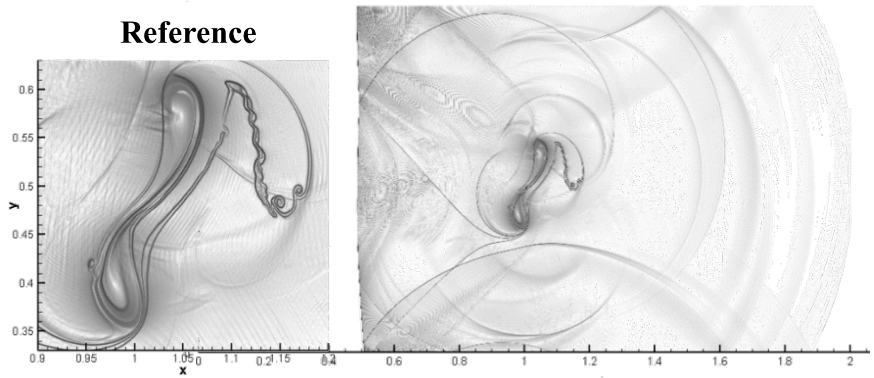

SNU1_P3_IT300

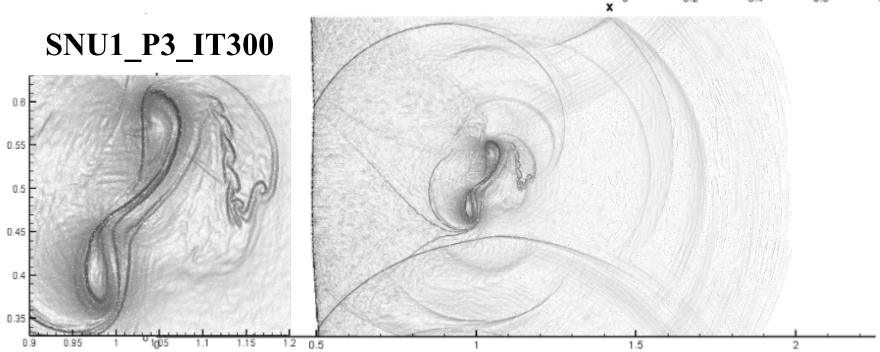

SNU1_P3_M300

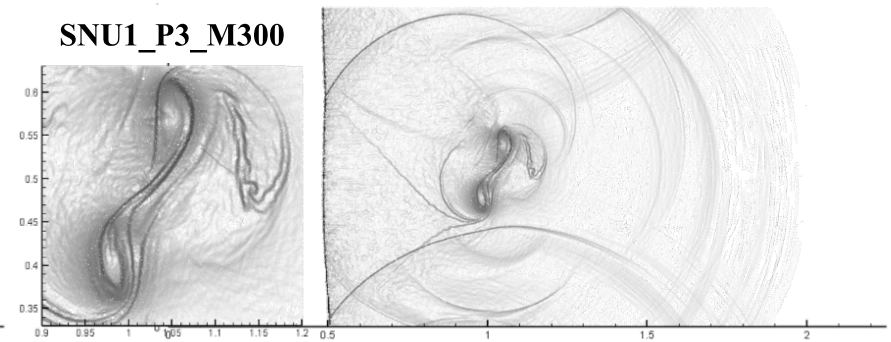

SNU1_P3_RQ300

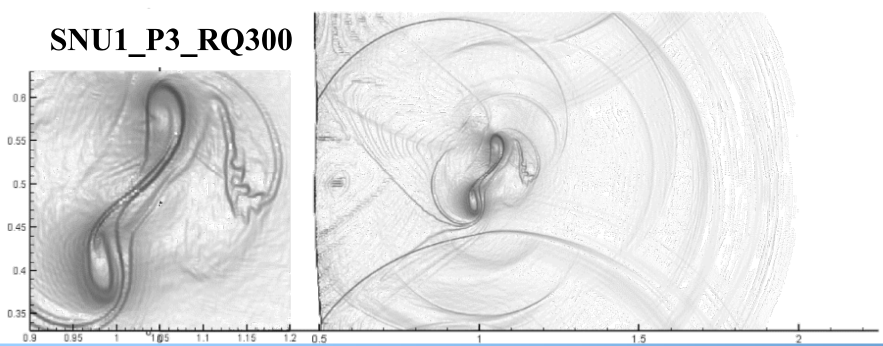

SNU1_P3_RT300

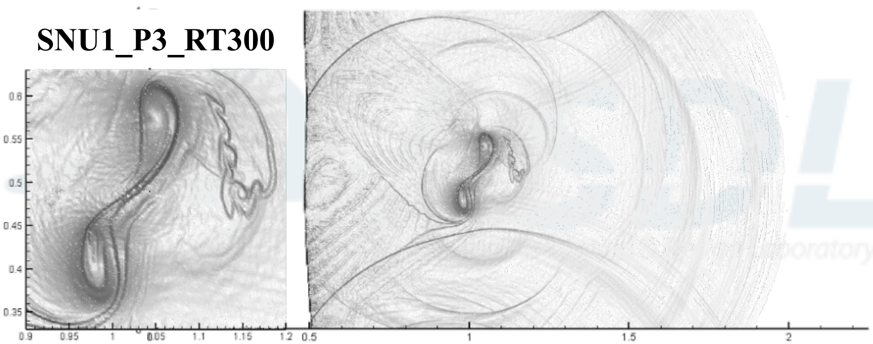

Results (Schlieren View)

- **Effects of grid size**

Reference

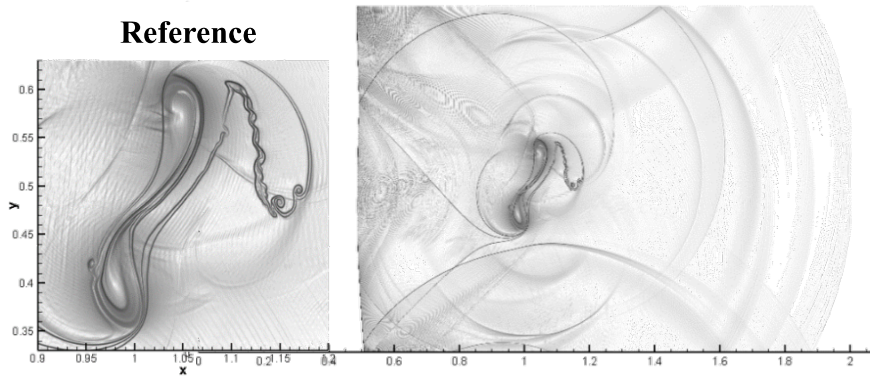

SNU2_P3_M50

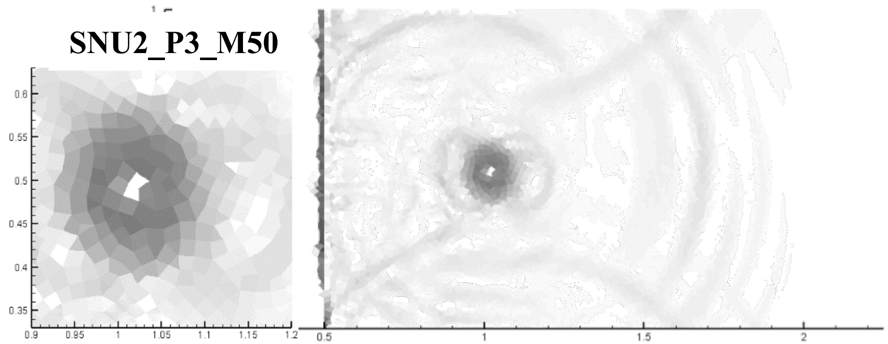

SNU2_P3_M100

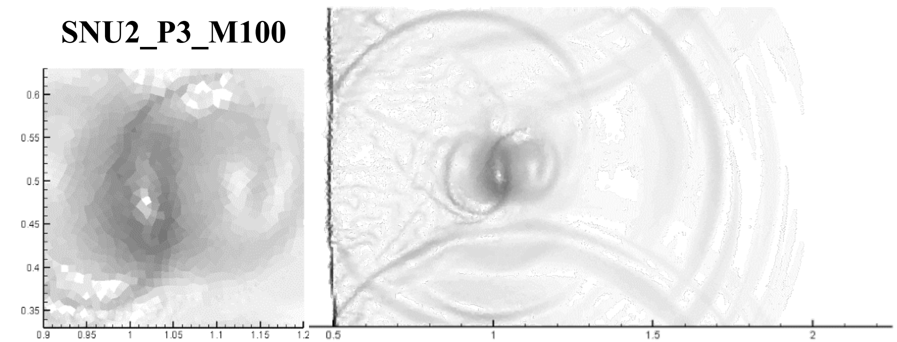

SNU2_P3_M200

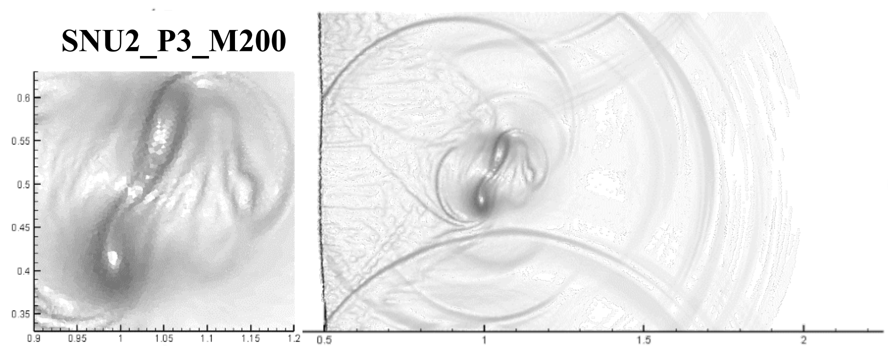

SNU2_P3_M300

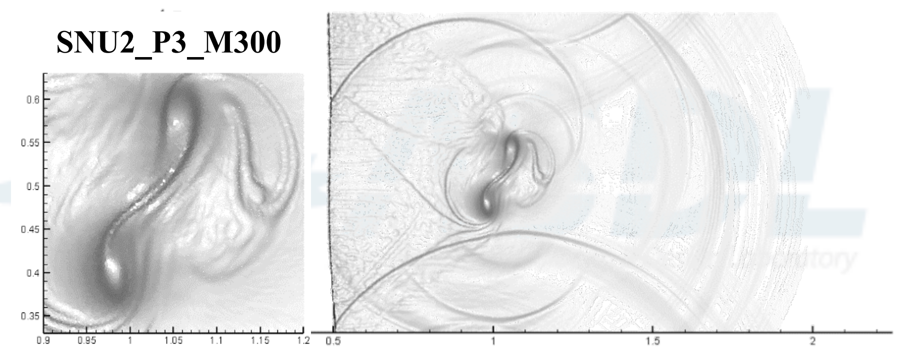

Results (Line 1)

- Well resolved large scale flow structure along Line 1

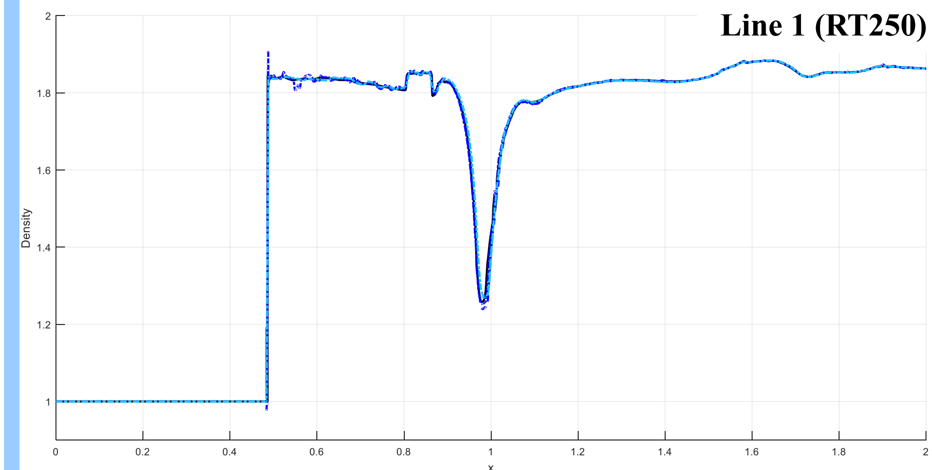

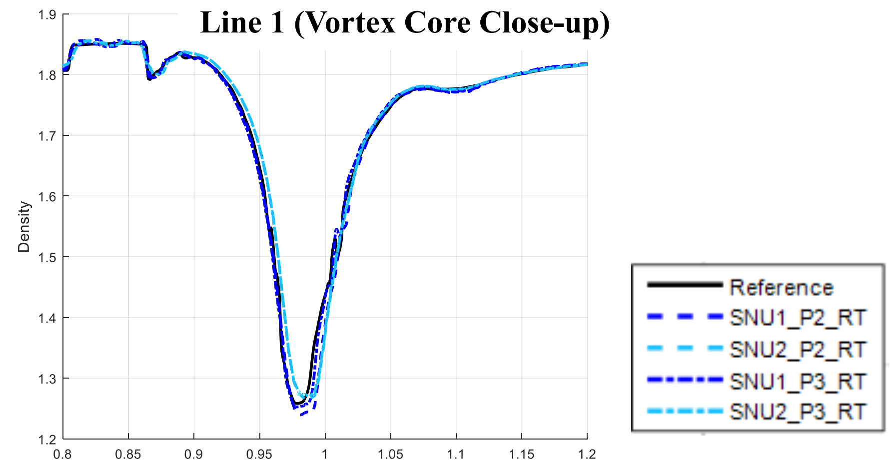

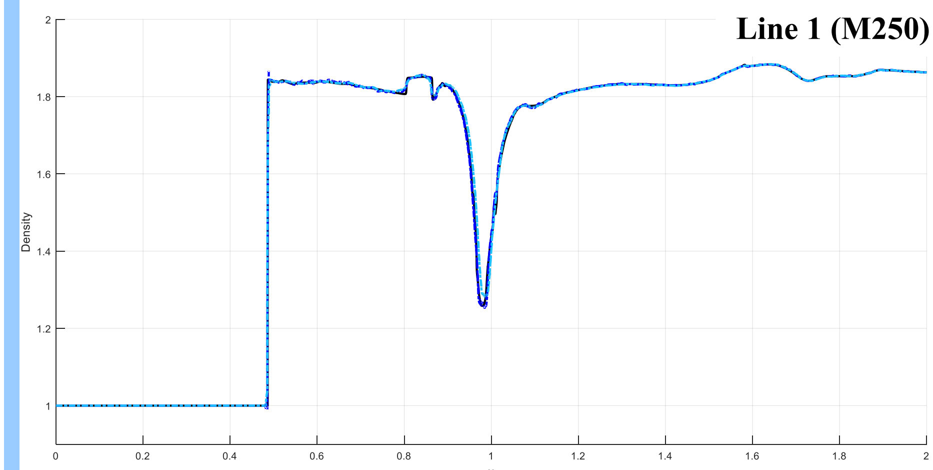

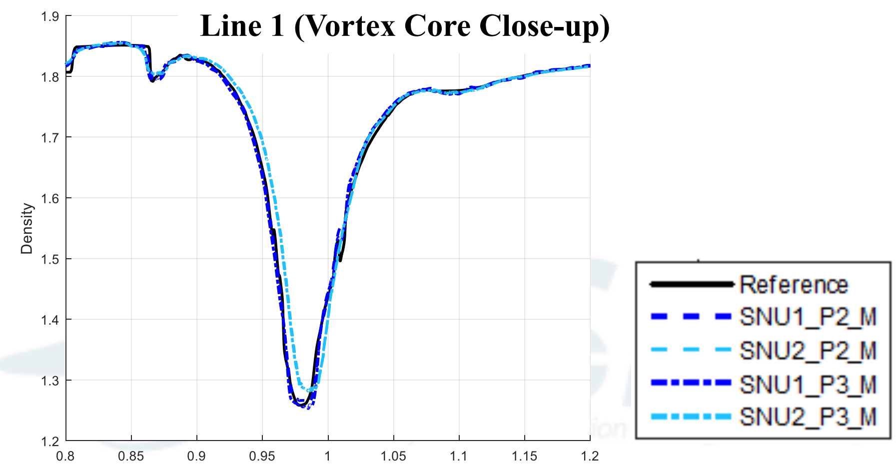

Results (Line 1)

- **Solution behavior around the stationary shock**
  - **Monotonicity is examined by total variation and maximum undershoot in [0.47, 0.5].**

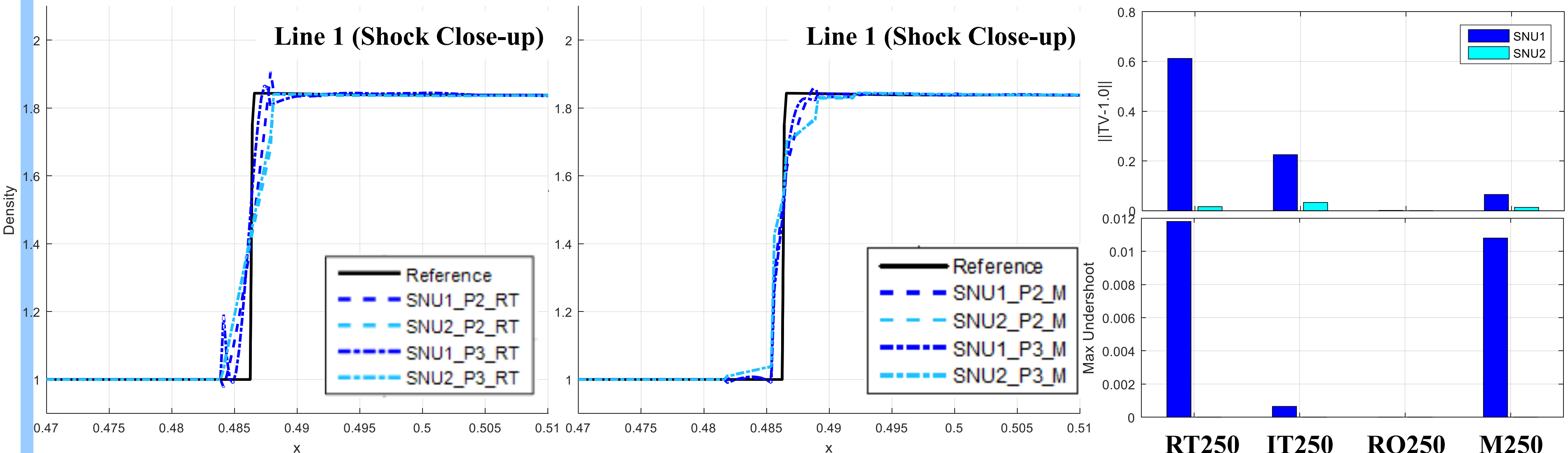

Comparison of Monotonicity across Shock ($P3$ approximation)

		SNU1_RT	SNU2_RT	SNU1_IT	SNU2_IT	SNU1_RQ	SNU2_RQ	SNU1_M	SNU2_M
$1/h$ =150	Total Variation*	1.082	0.9857	1.022	1.010	1.099	0.9942	1.242	1.092
	Max Undershoot*	6.799E-3	1.654E-6	5.059E-8	2.664E-7	7.077E-3	3.460E-7	4.649E-2	3.651E-7
$1/h$ =250	Total Variation*	1.612	0.9838	1.225	1.033	0.9995	1.000	1.065	0.9868
	Max Undershoot*	1.180E-2	8.277E-7	6.475E-4	2.213E-8	4.082E-11	1.254E-7	1.081E-2	6.986E-7

*: normalized by the shock strength ($\Delta\rho \approx 8.620\times10^{-1}$)

Results (Line 1)

- **Computation of error and order-of-accuracy along Line 1**
  - **Post-shock region ($x \geq 0.9$) is considered to compute errors with reference solution.**

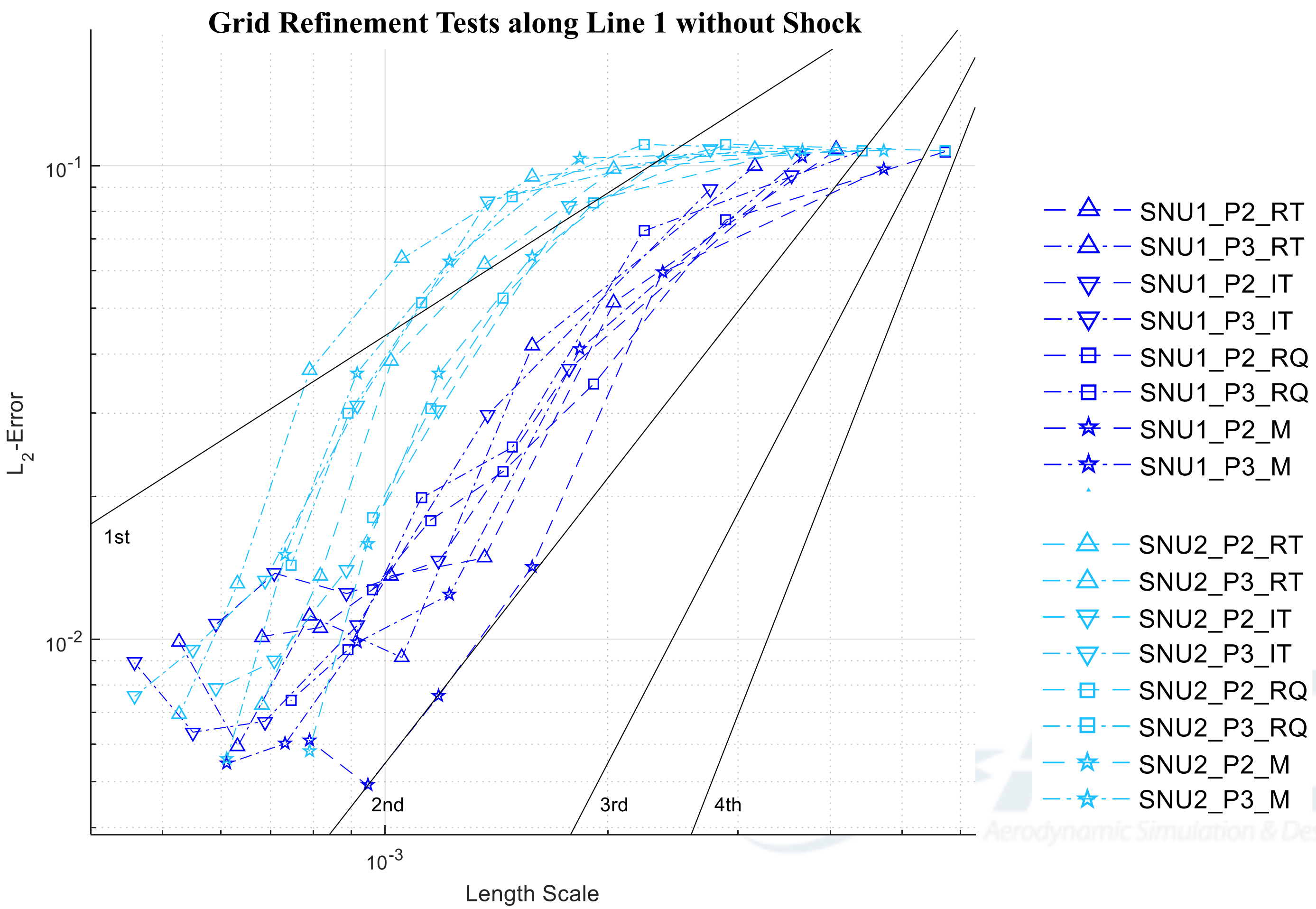

- Well resolved large scale flow structure along Line 2
- Monotonicity across the stationary shock

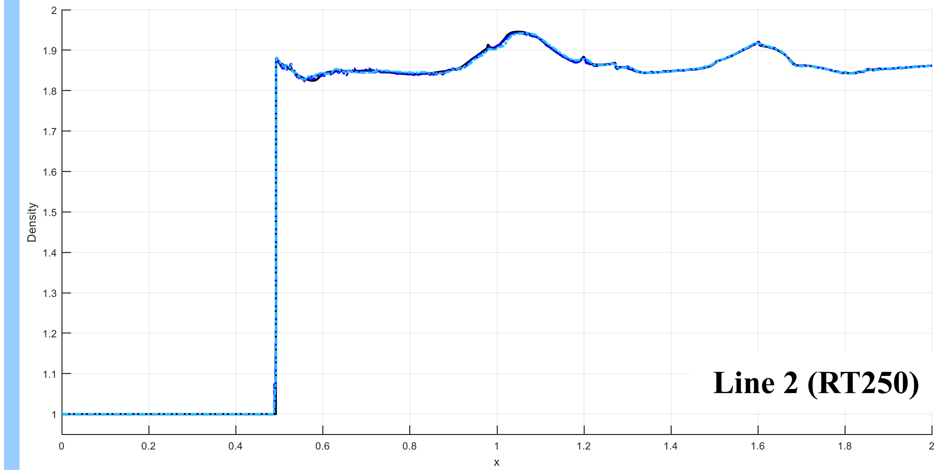

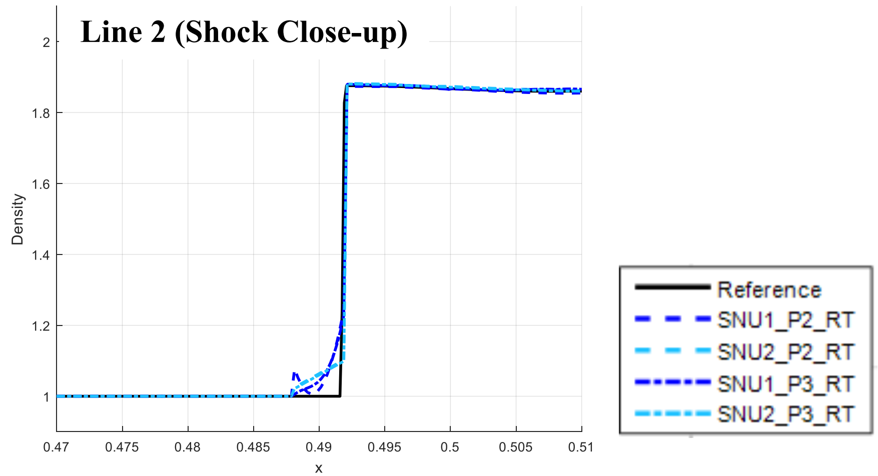

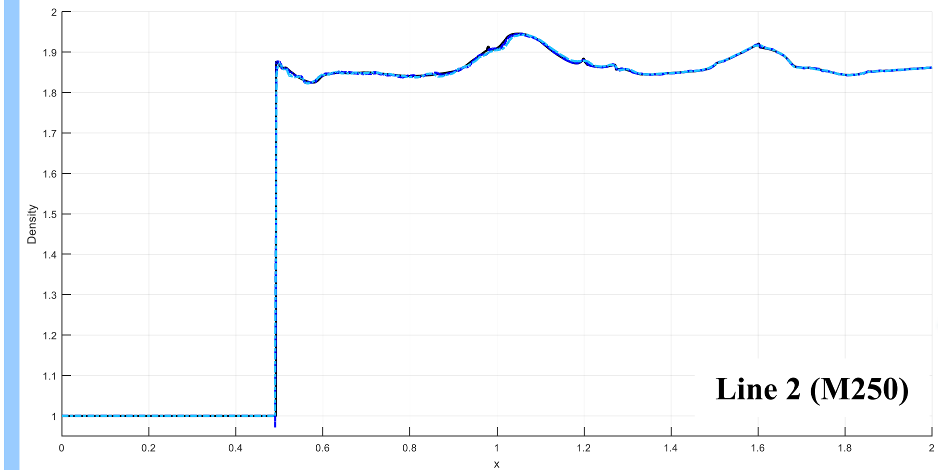

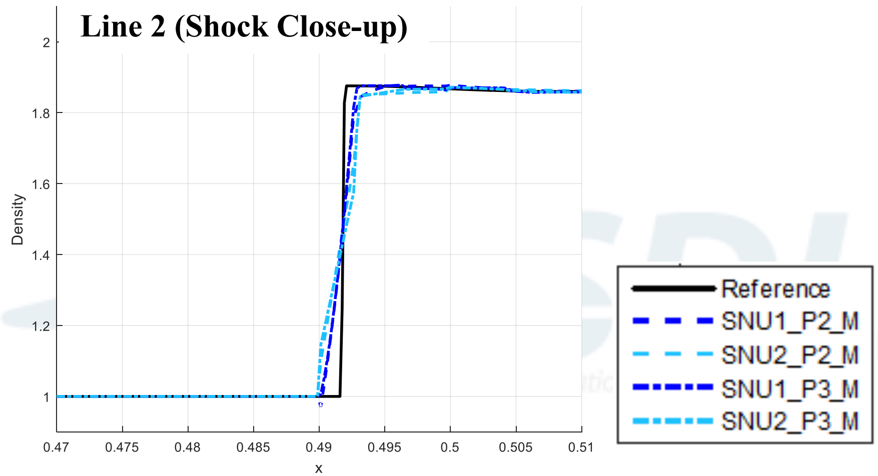

Results (Line 3)

- **Shock-driven oscillations along Line 3**
  - **Oscillations are examined by total variation and maximum difference in [0.2, 0.6].**

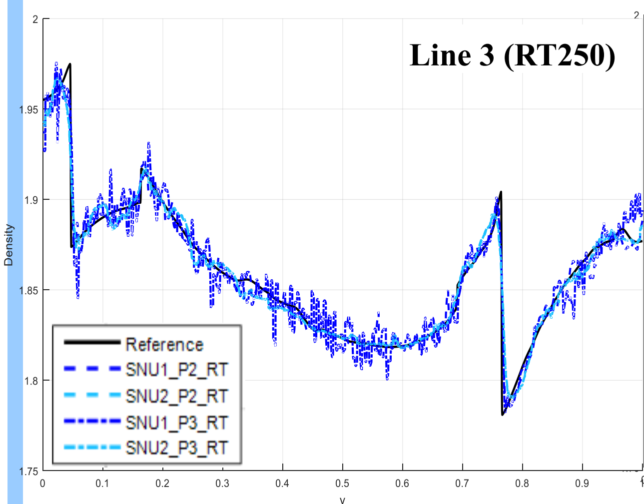

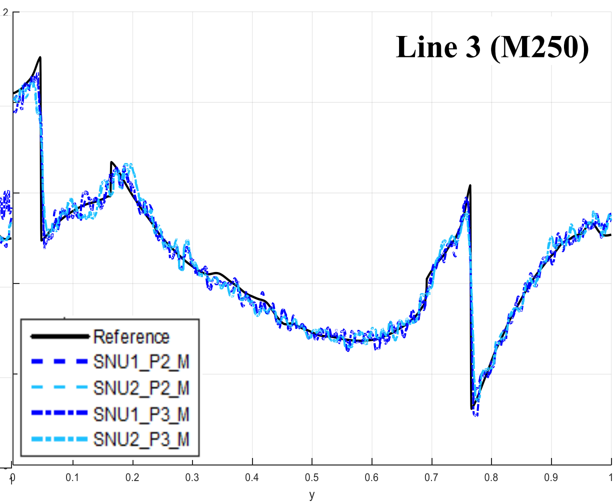

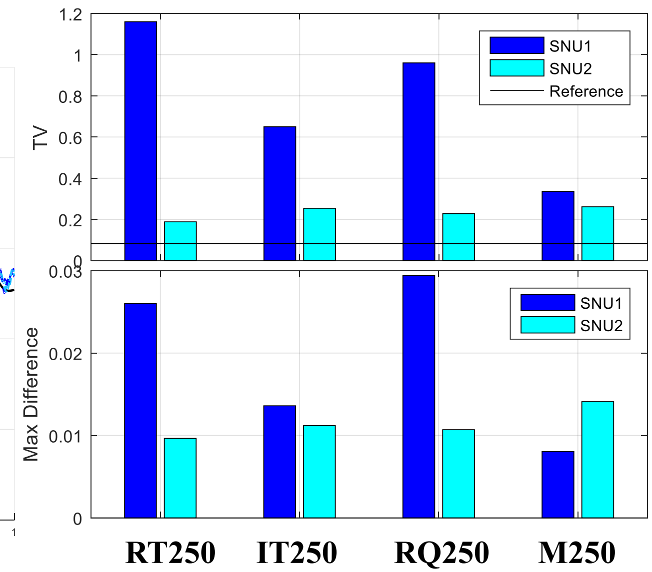

Comparison of Oscillations (*P*3 on 1/*h* =250 meshes)

	SNU1_RT	SNU2_RT	SNU1_IT	SNU2_IT	SNU1_RQ	SNU2_RQ	SNU1_M	SNU2_M
Total Variation*	1.163E+0	1.884E-1	6.496E-1	2.540E-1	9.598E-1	2.281E-1	3.363E-1	2.612E-1
Max Difference	2.601E-2	9.642E-3	1.364E-2	1.116E-2	2.938E-2	1.074E-2	8.054E-3	1.411E-2

***: Reference total variation is 8.270E-2**

- Vortical structure along Line 4

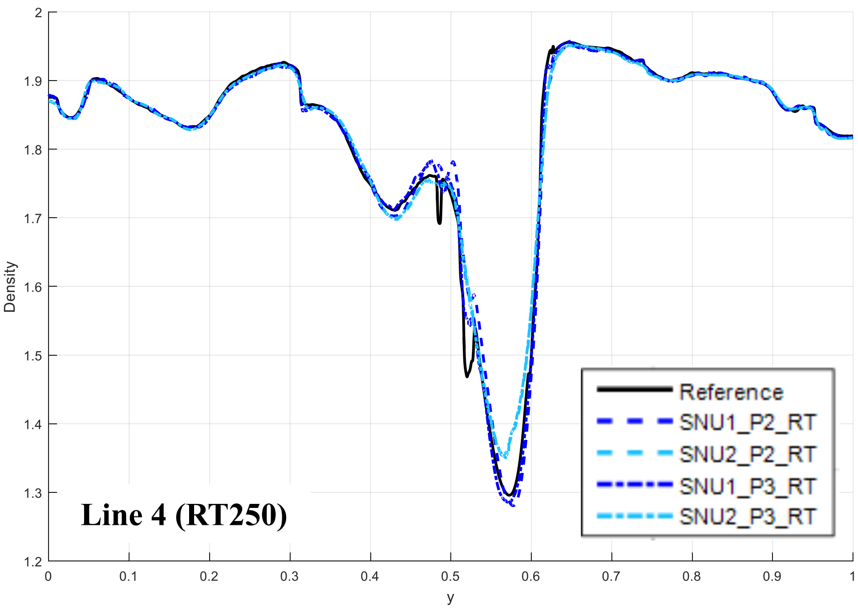

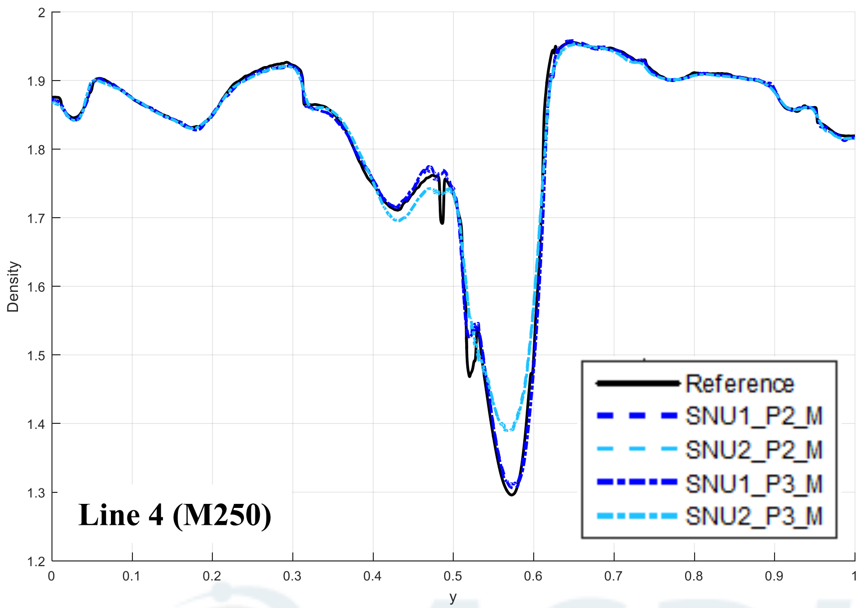

- Solution behavior and order-of-accuracy along Line 5 at far downstream region

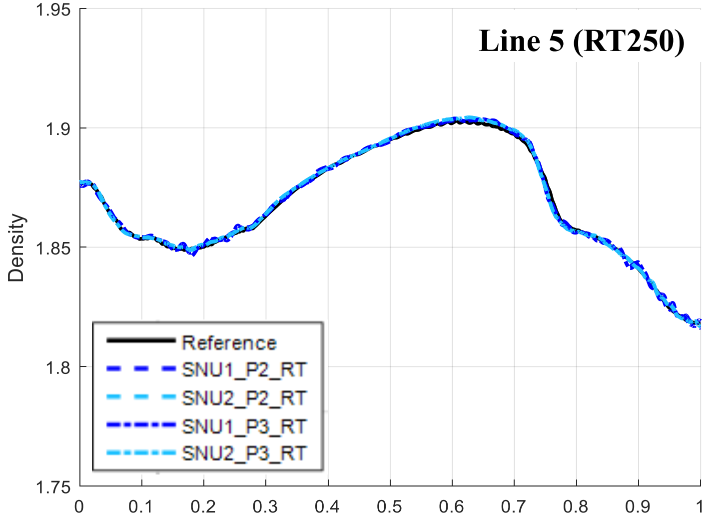

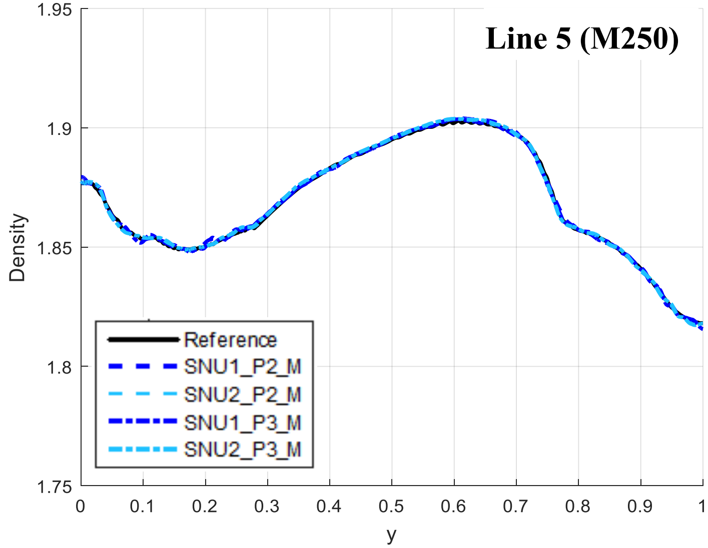

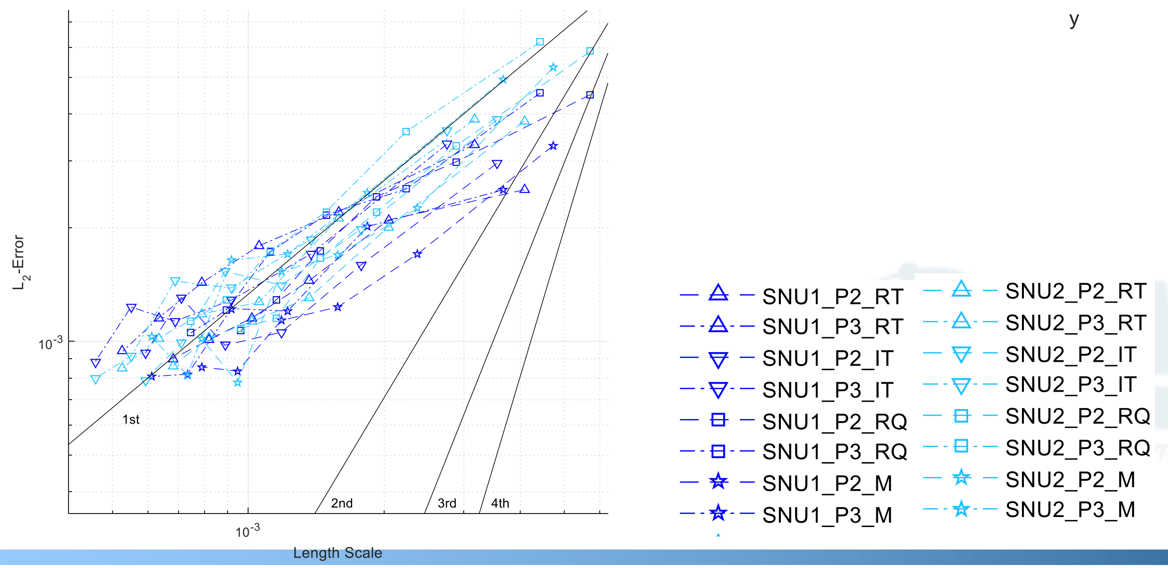

Experience

- **Examination of shock-capturing methods; *h*MLP vs *h*MLP_BD**

	*h*MLP	*h*MLP_BD
Subcell monotonicity across discontinuities	X	O
Required numerical diffusion	O	X
Mesh-type independency	X	O
Consistent behavior in order-of-accuracy	X	O

- **Difficulties**
  - **Shock-driven oscillations**
    - Pollute downstream flow field
    - Dependent on mesh-type, shock-mesh alignment, limiting strategy and numerical flux
  - **Degradation of accuracy in complex non-linear problems**
    - Possible factors are non-smooth initial profile, aliasing and inherent defection of numerical schemes.

References

[1] J.S. Park and C. Kim. "Higher-order multi-dimensional limiting strategy for discontinuous Galerkin methods in compressible inviscid and viscous flows." *Computers & Fluids* 96 (2014): 377-396.

[2] H. You and C. Kim. "Higher-Order Multi-Dimensional Limiting Strategy for Subcell Resolution." *23rd AIAA Computational Fluid Dynamics Conference*. 2017.

[3] H. You and C. Kim. "Higher-Order Multi-Dimensional Limiting Strategy for Subcell Resolution on Mixed Meshes." *14th US National Congress on Computational Mechanics*. 2017.